HHS Public Access

Author manuscript

Acta Biomater. Author manuscript; available in PMC 2021 May 01.

Published in final edited form as:

Acta Biomater. 2020 May ; 108: 67–76. doi:10.1016/j.actbio.2020.03.015.

A Liposome/Gelatin Methacrylate Nanocomposite Hydrogel System for Delivery of Stromal Cell-Derived Factor-1<alpha> and Stimulation of Cell Migration

Justine R. Yu[a,b,c], **Miriam Janssen**[a], **Barry J. Liang**[a], **Huang-Chiao Huang**[a,d], **John P. Fisher**[a,b,*]

[a]Fischell Department of Bioengineering, University of Maryland – College Park, 3121 A. James Clark Hall, 8278 Paint Branch Drive, College Park, MD 20742, USA

[b]NIH/NBIB Center for Engineering Complex Tissues, University of Maryland – College Park, 3121 A. James Clark Hall, 8278 Paint Branch Drive, College Park, MD 20742, USA

[c]University of Maryland School of Medicine Baltimore, MD 21201, USA

[d]Marlene and Stewart Greenebaum Cancer Center, University of Maryland School of Medicine Baltimore, MD 21201, USA

Abstract

Chronic, non-healing skin and soft tissue wounds are susceptible to infection, difficult to treat clinically, and can severely reduce a patient's quality of life. A key aspect of this issue is the impaired recruitment of mesenchymal stem cells (MSCs), which secrete regenerative cytokines and modulate the phenotypes of other effector cells that promote healing. We have engineered a therapeutic delivery system that can controllably release the pro-healing chemokine stromal cell derived factor-1α (SDF-1α) to induce the migration of MSCs. In order to protect the protein cargo from hydrolytic degradation and control its release, we have loaded SDF-1α in anionic liposomes (lipoSDF) and embedded them in gelatin methacrylate (GelMA) to form a nanocomposite hydrogel. In this study, we quantify the release of SDF-1α from our hydrogel system and measure the induced migration of MSCs *in vitro* via a transwell assay. Lastly, we evaluate the ability of this system to activate intracellular signaling in MSCs by using Western blots to probe for the phosphorylation of key proteins in the mTOR pathway. To our knowledge, this is the first study to report the delivery of liposomal SDF-1α using a nanocomposite approach. The results of this study expand on our current understanding of factors that can be modified to affect MSC behavior and phenotype. Furthermore, our findings contribute to the development of new hydrogel-based therapeutic delivery strategies for clinical wound healing applications.

*Corresponding author jpfisher@umd.edu.

6.Disclosure

The authors have no competing interests to declare.

Graphical Abstract

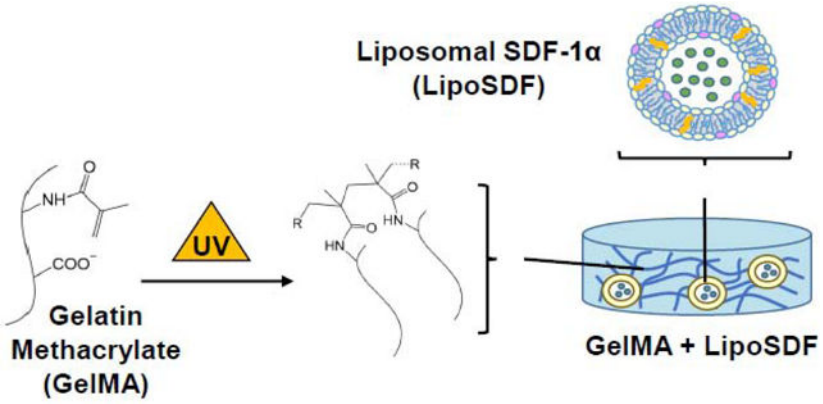

Keywords

Liposome; nanocomposite hydrogel; mesenchymal stem cell; migration

1. Introduction

Non-healing skin ulcers are a common complication in patients suffering from chronic conditions such as diabetes and peripheral vascular disease, or in situations where sustained pressure compromises local circulation (i.e. decubitus ulcers) [1,2]. While mild to moderate cases are typically managed with non-surgical methods, severe wounds may warrant the use of tissue engineered skin substitutes to address wound defects and stimulate healing, especially if skin grafting techniques are limited by other comorbid conditions [3–5]. Such constructs may further incorporate exogenous proteins or small molecule drugs in order to locally accelerate wound closure and facilitate tissue regeneration [6,7].

Chronic wounds are characterized by an inflammatory environment that impairs the recruitment of mesenchymal stem cells (MSCs), which play an important role in directing the progression of normal healing mechanisms that lead to wound closure and skin tissue regeneration [8]. These MSCs normally migrate in response to chemotactic factors secreted by cells at the wound site, where they in turn produce immunomodulatory and pro-healing cytokines [9]. Towards this end, we seek to develop a nanocomposite hydrogel to tune the release kinetics of a pro-healing chemokine such as stromal cell derived factor-1α (SDF-1α, also known as CXCL12) over a physiologically relevant timespan. SDF-1α is a protein constitutively produced by endothelial cells, pericytes, and dermal fibroblasts, and upregulated when there is injury [10]. This protein has been previously used in tissue regeneration and vascular remodeling applications due to its ability to stimulate cell migration and promote pro-healing behavior in anti-inflammatory subsets of monocytic immune cells [11–14]. Furthermore, SDF-1α is also known to facilitate the mobilization of MSCs from the bone marrow, which in turn secrete anti-inflammatory, pro-healing cytokines or are phagocytosed by macrophages to induce phenotypic changes (a process known as efferocytosis) [15–17]. Previous studies have successfully utilized engineered hydrogel or

thin film systems to deliver SDF-1α in applications such as promoting cell homing to cardiac tissue and supporting angiogenesis or myogenesis [12,13,18].

However, the direct delivery of therapeutic agents is often hampered by rapid diffusion and (in the case of growth factors and chemokines) the activity of proteolytic enzymes, which are especially prevalent in chronic inflammatory environments [19]. Furthermore, hydrogel delivery systems composed of natural, extracellular matrix- (ECM-) derived materials tend be mechanically fragile and degrade quickly *in vivo* [20]. Thus a major challenge to the local delivery of proteins is the need to maintain controllable release at therapeutically effective concentrations while minimizing the loss of the protein cargo by proteolytic degradation or passive diffusion [21,22].

Nanocomposite hydrogels are composed of nanostructures or nanoparticles that physically interact with crosslinked polymer chains in a hydrogel network [23–25]. Liposomes in particular are an attractive option for this strategy due to their biocompatibility and tunability in protecting and delivering protein or small molecule cargos across a wide range of physical properties [24,26]. However, on their own, nanoscale substances such as liposomes and their cargo diffuse away quickly from the site of administration, effectively decreasing the therapeutic concentration at the injury site [23,24]. In order to achieve a longer rate of localized release, liposomes may be combined with a hydrogel, which serves to physically sequester the encapsulated material within the construct and aids in sustaining release at concentrations high enough to stimulate physiological activity [23].

In this work, we develop a nanocomposite liposome/gelatin methacrylate (GelMA) hydrogel system to generate a localized, sustained release of SDF-1α capable of inducing migration and phenotypic changes in MSCs. We hypothesize that SDF-1α may be stably incorporated in anionic liposomes and further embedded in a negatively charged, Type B GelMA hydrogel (Figure 1), which contain protease-sensitive motifs but also chemical crosslinks that preserve mechanical stability [20]. As the protein is released from the liposomes, it is then sequestered within the hydrogel network via electrostatic interactions with polymer chains, which slows its diffusion into the periphery. The objectives of our work are to demonstrate that the delivery system that we have developed is capable of controllably releasing SDF-1α, that the protein is released at concentrations that effectively induce MSC migration, and that this released chemokine is bioactive and capable of exerting an effect on intracellular cell signaling pathways in MSCs.

2. Materials and methods

2.1. GelMA synthesis and hydrogel preparation

We have adapted protocols previously published by our group to synthesize GelMA polymer [27,28]. Briefly, Type B gelatin (225 Bloom from bovine skin, Sigma) was dissolved in phosphate buffered saline (PBS) at 0.1 g/mL. Methacrylic anhydride (MA, Sigma) was then slowly added dropwise at a proportion of 0.6 g MA/1 g gelatin, and the solution was allowed to react for 1 hour. Afterwards, the mixture was diluted and dialyzed against deionized water for 72 hours, adjusted to a pH of 7.4, and frozen at −80 °C before lyophilization for another 72 hours. This procedure yielded a porous foam that was stored at −80 °C until use. GelMA

hydrogels were formed by dissolving lyophilized GelMA in PBS with 0.1% w/v lithium phenyl-2,4,6trimethylbenzoylphosphinate (LAP, Tocris) at 50 °C. 200 μL of the resulting mixture was then pipetted into 8 mm-diameter cylindrical molds and placed at 4 °C for 20 minutes to allow for soft gelation. Afterwards, the gels were exposed to UV light for 2 minutes in a UV box to photocrosslink.

2.2. Nuclear magnetic resonance (NMR) spectroscopy

1H NMR (Bruker AVIII-600 MHz) was used to verify the addition of vinyl groups from the methacrylation reaction. Lyophilized GelMA polymer was dissolved in deuterium oxide (−) at a concentration of 10 mg/mL, and samples were run at 40 °C. Data was analyzed using Bruker TopSpin3.5 software.

2.3. Assessment of hydrogel degradation

To assess the rate of enzymatic degradation, GelMA hydrogels (7.5, 10, and 15% w/v) were incubated at 37 °C in 16 μg/mL collagenase IV (EMD Millipore) for up to 1 week. At each time point, hydrogels were collected, lyophilized, and massed. Degradation rate was determined by calculating the mass remaining at each time point using the following formula:

$$\text{Mass remaining } (\%) = (m_0 - m_t)/m_0 \times 100$$

where m_0 is the initial dry weight of undigested samples and m_t is the dry weight of digested samples at each time point [29].

2.4. Rheology

GelMA was cast into cylindrical molds to form 1 mL-hydrogels for oscillatory rheological testing (ARES-G2, TA Instruments). Hydrogels were placed between a set of parallel plates and subjected to a frequency sweep between 0.1–10 rad/s with a constant strain of 0.1%. Rheological studies conducted on swollen samples were conducted after soaking the hydrogels in PBS overnight.

2.5. Liposome synthesis and protein loading

Adapting procedures described by our group and others [30–35], anionic liposomes were formed by dissolving ovine wool cholesterol in chloroform (10 mg/mL, Sigma) and combining it with 10 mg/mL each of 1,2-distearoyl-sn-glycero-3-phosphocholine (DSPC, Avanti Polar Lipids) and 1,2-dioctadecanoyl-sn-glycero-3-phospho-(10-rac-glycerol) (sodium salt) (DSPG, Avanti Polar Lipids) at a molar ratio of 25:65:10. The 1 mL mixture was placed on a rotovap overnight (Büchi R-100) at 40 °C and 100 mBar to remove the chloroform and generate a thin lipid film, which was subsequently rehydrated with 1 mL SDF-1α solution in PBS (12.5 μg/mL, Peprotech). This solution was vortexed to form an emulsion and extruded 10 times through a polycarbonate filter with a pore size of 200 nm (Whatman) at 55 °C to produce liposomes of uniform size. Before use in experiments, liposomes were dialyzed against PBS at 4 °C in a Float-A-Lyzer G2 dialysis device with a 300 kD cutoff (Repligen) overnight to remove unencapsulated protein.

2.6. Liposome characterization

The hydrodynamic diameter, polydispersity index (PdI), and zeta potential of fresh liposomes were measured at 25 °C by dynamic light scattering (DLS) and electrophoretic light scattering (ELS) with the NanoBrook Omni particle size and zeta potential analyzer (Brookhaven Instruments). 5 μL of the liposome suspension was diluted in 2 mL of ultrapure water for DLS or 1.5 mL of 1 mM NaCl for ELS. Measurements were then repeated for up to 2 weeks to examine particle stability at 4 °C.

Encapsulation efficiency (EE%) was determined by sampling the liposome suspension before dialysis and quantifying the amount of unencapsulated SDF-1α by ELISA (Peprotech) following the manufacturer's protocols. EE% was then indirectly calculated by the following formula:

$$EE\% = (m_i - m_d)/m_i \times 100$$

where m_i is the initial mass of SDF-1α used in film rehydration and m_d is the mass of unencapsulated SDF-1α detected by ELISA.

Cryo-transmission electron microscopy (cryo-TEM) images were obtained using the JEM-2100 LaB6 TEM (JEOL) at the Advanced Imaging and Microscopy Laboratory at the Maryland NanoCenter. Scanning electron microscopy (SEM) with ionic liquid treatment was conducted using the SU-70 Field Emission SEM (Hitachi).

2.7. Characterization of SDF-1α release

To characterize protein release from liposomes, 500 μL of fresh liposomal SDF-1α (lipoSDF) suspension was added to the top chamber of a Slide-A-Lyzer MINI Dialysis device (20k MWCO, Thermo Fisher) and dialyzed against PBS for one week at 37 °C. At each time point, a 50 μL sample was taken and centrifuged at 1500 g for 30 minutes at 4 °C to separate the liposomes from the released protein. The supernatants were then transferred into separate tubes for analysis by ELISA to determine the amount of SDF-1α released.

To assess the ability of SDF-1α to be released from within the GelMA matrix over time, 5 μg/mL of SDF-1α or lipoSDF was added to GelMA solutions before crosslinking. Samples were incubated in PBS/0.1% BSA for 1 week at 37 °C in the presence of 16 μg/mL collagenase IV. At each time point, supernatants were collected from each sample and replaced with fresh solution. The cumulative release of SDF-1α into these supernatants was then assessed by ELISA as before.

2.8. Cell culture

Human bone marrow-derived MSCs (RoosterBio) were expanded in RoosterNourish media (RoosterBio) until confluency and used up to passage 8. Cells were seeded at 1×10^5 cells/well for transwell experiments and 2.5×10^5 cells/well for Western blot experiments. In both cases, MSCs were first serum-starved overnight in Dulbecco's Modified Eagle Medium (DMEM, Thermo Fisher) before seeding the following day.

2.9. Transwell migration assay

MSCs were seeded in the top chamber of 24-well transwell inserts (Millipore Sigma) and allowed to migrate towards the bottom chamber containing DMEM conditioned by either PBS, 80 ng/mL free SDF-1α, or lipoSDF (containing 80 ng/mL SDF-1α as determined by ELISA). After 24 hours, unmigrated cells on the apical surface of the membrane were removed with a cotton tip. The membranes were then stained with Hoechst 33342 nuclear stain (5 ng/mL, Thermo Fisher), and imaged under fluorescence microscopy. Nikon NIS-Elements analysis software was used to count the number of migrated cells in a total of 5 random fields of view per sample. In a similar fashion, GelMA containing 5 μg/mL of SDF-1α or lipoSDF was used to condition DMEM over 1 week. This media was collected at each time point and used to stimulate MSC migration for 2 hours before staining and counting.

2.10. Western blotting

Media was conditioned over 1 week by GelMA containing 5 μg/mL of SDF-1α or lipoSDF as detailed above. MSCs were then exposed to conditioned media for 2 hours before lysis with RIPA buffer (Thermo Scientific) containing a cocktail of phosphatase and protease inhibitors (Abcam). Lysates were then mixed with Laemmli buffer (Bio-Rad) and run on a 12% SDS/PAGE electrophoresis gel before being transferred onto a nitrocellulose membrane using a Trans Blot semi-dry transfer machine (Bio-Rad). Membranes were then probed with primary rabbit antibodies against human AKT p473, RPS6 pS235/236 (1:250 dilution, Abcam), as well as total AKT and RPS6 (1/500, 1/5000, Abcam). A secondary horseradish peroxidase-conjugated goat anti-rabbit antibody (1:10,000 dilution, Abcam) was used in conjunction with enhanced chemiluminescence substrate (Bio-Rad) to visualize the protein bands.

2.11. Statistical Methods

Unless noted, data is presented as mean ± STD with n = 3 biological replicates per group. Depending on the comparisons being made, a Student's T-test or one-way analysis of variance (ANOVA) with Tukey's *post hoc* test was used to determine statistical differences between groups, with $p < 0.05$ considered to be significant. Statistical analyses were conducted using Minitab 18.

3. Results

3.1. Characterization of GelMA hydrogels

The reaction of methacrylic anhydride with Type B gelatin to form GelMA was confirmed by 1H NMR spectroscopy by assessing for the presence of vinyl groups in the sample spectrums. A pair of peaks was observed between 5.5 – 6 ppm, corresponding to the protons from the vinyl group of methacrylate (Figure 2A, blue spectrum) [36,37]. These peaks were not present in the NMR spectrum of gelatin (red spectrum).

GelMA hydrogels digested in collagenase IV solution were collected at each time point, lyophilized, and massed in order to determine their rates of degradation (Figure 2B). This

produced a content-dependent trend with slower degradation as GelMA content was increased (*p < 0.005, **p < 0.001).

Rheology conducted on GelMA + lipoSDF hydrogels showed that for all concentrations of GelMA used, the storage modulus (G') was greater than the loss modulus (G") across the entire frequency range (Figure A.1.). This effect was observed in both newly-fabricated hydrogels and as well as gels that were allowed to swell in PBS overnight.

3.2. Characterization of liposomes

Unilamellar empty liposomes (lipo) and lipoSDF were formed with a hydrodynamic diameter of 227 ± 5 and 236 ± 3 nm, respectively, and with a narrow size distribution (PdI < 0.1) (Figures 3A and 3C). The diffusion coefficients of lipo and lipoSDF particles was measured to be 2.1 and 2.0×10^{-8} cm^2/s respectively in water, which when compared against the diffusion coefficient of free SDF-1α protein (1×10^{-6} cm^2/s) [38], indicates that these larger particles are slower to diffuse in the medium [39]. In order to minimize the destabilizing electrostatic interactions between the liposomes and the negatively charged GelMA, the surface charge of the liposomes was engineered to have a slight negative charge between −48 and −41 mV, as measured by ELS (Figure 3E). To determine the encapsulation efficiency of lipoSDF, an ELISA assay was conducted to determine the protein concentration in lipoSDF after dialysis and compared the amount that was added initially. Passive loading of SDF-1α into liposomes resulted in an encapsulation efficiency of 88 ± 6%. Lastly, the hydrodynamic diameter and zeta potential of the same batch of lipoSDF was monitored for 2 weeks to assess for particle stability (Figure A.2.). Narrow distributions were observed in both with minimal changes over time, suggesting that these particles remain stable over time when stored at 4 °C.

3.3. Release of SDF-1α from liposomes and GelMA

LipoSDF was shown to follow burst release kinetics over 1 week (Figure 4A), while hydrogel-loaded, unencapsulated SDF-1α was released more slowly and as a function of GelMA concentration (Figure 4C). When applied to well-known models of drug release, the GelMA + SDF profiles were found to readily fit the Korsmeyer-Peppas model ($0.97 \leq r^2$, Figures 4D and A.3.A):

$$M_t / M_\infty = K_{KP} t^n$$

where M_t / M_∞ is the fraction of released drug at time t, K_{KP} is the Korsmeyer-Peppas rate constant, and n is the release exponent that identifies the mechanism of drug release [40].

When GelMA hydrogels were loaded with lipoSDF, however, the release followed more exponential profiles (Figure 4E). These release curves did not fit the Korsmeyer-Peppas model (Figures A.3.B and A.3.C), but were found to fit the Weibull model of delayed release instead ($0.96 \leq r^2$, Figure 4F):

$$M_t/M_\infty = 1 - \exp\frac{-(t - T_i)^\beta}{\alpha}$$

where M_t / M_∞ is the fraction of released drug at time t, T_i is the delay time before the start of release, α is the scale parameter, and β is the shape parameter [41,42].

3.4. Transwell migration assays

MSCs seeded on transwells were exposed to serum-free media conditioned by 80 ng/mL of either SDF-1α or lipoSDF. Both groups were able to significantly induce more chemotaxis of MSCs compared to the negative control of DMEM supplemented only with PBS ($p < 0.01$, Figures 5A and 5B). This suggests that our lipoSDF fabrication method does not impair the ability of the chemokine to induce MSC migration.

MSC migration was assessed over 1 week in response to media conditioned by 10% GelMA + SDF or 10% GelMA + lipoSDF. At each time point, conditioned media was collected to stimulate MSCs for 2 hours before they were stained and counted. Increased migration was observed at Days 3 and 7 in the GelMA + lipoSDF group, while no such trend was observed with GelMA + SDF ($p < 0.05$, Figure 5C).

3.5. Western blots to assess for mTOR signaling activity

Western blots for phosphorylated (phospho-) AKT and RPS6 demonstrated that our GelMA + SDF and GelMA + lipoSDF constructs are capable of exerting effects on the phosphorylation status of key signaling proteins from the mammalian target of rapamycin (mTOR) pathway (Figure 6A). Densitometry analysis indicated that for AKT, the trends of mean intensity of the GelMA + lipoSDF group were lower (means < 1) than the negative PBS-treated control on all days, while the GelMA + SDF group did not show this effect (Figure 6B). For RPS6, both groups showed decreasing levels of protein over time (means < 0.91 by Day 7) below both the negative PBS control and the positive control of soluble SDF-1α (Figure 6C).

4. Discussion

In this work, we have developed a nanocomposite hydrogel delivery system capable of releasing the chemokine SDF-1α in liposomal form and demonstrated that this system can affect cell signaling processes and induce chemotaxis in MSCs for up to 1 week. Similar nanocomposite constructs have previously been leveraged to control the delivery of therapeutic proteins such as PlGF, MCP-1, and EGF [42,43]. The use of liposomes for these applications is particularly attractive due to the high hydrophilicity of charged proteins such SDF-1α, which are thought to interact minimally with the hydrophobic membrane and allow for more efficient incorporation into the aqueous core [44–47]. For our work, we opted to use an anionic liposome formulation to minimize any electrostatic attraction between the liposomes and the negatively charged GelMA that could cause the hydrogel fibers to insert in the lipid bilayer and destabilize the particles [48]. We chose to use this strategy in particular because proteins such as SDF-1α are susceptible to enzymatic degradation, and

this method provides an additional method of locally concentrating the protein and isolating it from nearby proteases compared to direct adsorption to a hydrogel [44,49].

As SDF-1α is a chemokine, one of the most important indicators of its activity is its ability to induce chemotaxis in nearby cells. In our study, we assessed the bioactivity of our released SDF-1α by measuring its ability to chemoattract MSCs. Furthermore, we studied the released protein's ability to exert effects on the mTOR pathway. This requires the presence of intact, unencapsulated protein that can bind to the cells' surface receptor CXCR4 and activate downstream signaling factors. By encapsulating SDF-1α within liposomes and further embedding them within GelMA hydrogels, we are able to deliver protein with preserved bioactivity for up to 1 week.

Our studies have demonstrated that our SDF-1α-loaded liposomes are monodisperse in solution and retain tight size and charge distributions even after 2 weeks at 4 °C (Figures 3 and A.2.). These findings suggest that our liposomes have a prolonged shelf-life, can be stably loaded in hydrogels, and will retain their therapeutic efficacy even after being stored for at least 2 weeks.

The use of GelMA in this application represents an innovative strategy to control the release of a liposomal encapsulated therapeutic protein. GelMA hydrogels contain matrix metalloproteinase- (MMP-) sensitive motifs that render them susceptible to enzymatic degradation (Figure 2B), but this rate is modifiable by changing the number of crosslinks between methacrylate groups [50]. In our rheological studies, we found that, for all concentrations of GelMA used, the G' of our GelMA + lipoSDF hydrogels was always greater than the G", indicating that our hydrogels tend to deform elastically rather than flow when shear is applied (Figure A.1.). We hypothesize that this is due to the highly structured nature of the hydrogel, which is extensively crosslinked throughout the network [51]. This helps to preserve some of the structure and mechanical properties of the hydrogel constructs as they naturally degrade over time, which is especially critical in the context of dressings for wound healing applications [1,7]. This effect was also observed after the hydrogels were fully swollen, which suggests that they can maintain mechanical stability in an aqueous environment.

One other application of GelMA is to tune the release kinetics of our protein of interest. Much like native skin ECM, which is mainly composed of Type I collagen, GelMA derived from alkaline-processed, Type B gelatin (itself a denatured form of collagen) carries a net negative charge [52]. Proteins such as SDF-1α, which contains a large number of basic amino acid residues such as lysine and hydroxylysine that contributing to its positive charge, will form electrostatic interactions with these hydrogel fibers [53]. This will slow its diffusion out of negatively charged gels and allow it to retain a relatively high local concentration that is physiologically relevant to nearby cells, including those that may eventually migrate into the gel itself [47,54]. We have shown that we are able to tune the release kinetics by encapsulating SDF-1α in liposomes and embedding them in a GelMA hydrogel; by using this method we are able to achieve faster and higher amounts of protein release in a time-delayed manner compared to using unencapsulated SDF-1α instead. Electrostatic interactions between Type Bderived GelMA and SDF-1α would account for the

attenuated burst release pattern in Figure 4C showing decreased amounts of SDF-1α release compared to that from loaded liposomes only (Figure 4A). Conversely, the use of anionic liposomes would prevent excessive electrostatic interactions between the lipid membranes and the GelMA fibers, which might otherwise destabilize the particles to cause earlier cargo release. The kinetics in Figure 4E reflect this decreased release in the first 1–3 days, with higher amounts of release in the subsequent days as the GelMA hydrogels degrade and protein is released from the nanoparticles. Furthermore, lipoSDF has a diffusion coefficient 2 orders of magnitude lower than free SDF-1α, leading to slower diffusion in aqueous environments. This may also play a role in the low release from GelMA + lipoSDF in the first 1–3 days. In comparison, the direct charge-charge interactions between the negatively charged Type B-derived GelMA and the positively charged SDF-1α causes the protein to remain complexed to the GelMA fibers and release slowly from the hydrogel over the entire time course.

We found that the release profiles of the GelMA + SDF groups could be modeled by the Korsmeyer-Peppas equation for diffusion-controlled drug release (Figure 4D). The calculated release exponent (n) for the 10% and 15% GelMA groups was about 0.5, indicating that these systems obey classic Fickian diffusion schemes, while the 7.5% GelMA group had an exponent that suggested anomalous, non-Fickian transport characterized by both time-dependent solute diffusion and swelling of the polymer matrix ($0.45 < n < 0.89$ and $n \neq 0.5$) [40,41]. Furthermore, we saw that only the GelMA + SDF, but not the GelMA + lipoSDF groups fit this model (Figure A.3.). Instead, the latter groups were more readily modeled as a delayed release system using the Weibull equation, whose shape parameter (β) can be used to describe the shape of the release profile (Figure 4F) [42]. For all GelMA + lipoSDF groups, $\beta < 1$, indicating that release from the system first occurs with a steep slope before following a more exponential shape [41]. We believe that this phenomenon occurs due to a small degree of leakage or burst release that results from some liposomes releasing their cargo at early time points [49]. This might result in SDF-1α being sequestered within the gel through charge-charge interactions that prevents diffusion away from the site until the GelMA hydrogel is degraded [12,18]. Alternatively, SDF-1α may be complexed with the negatively charged DSPG lipids on the liposome surface, causing any liposomes outside the gel to be detected by our antibody-based detection assays.

As our modeling attempts indicate that SDF-1α could diffuse from our system in a manner describable by Fick's laws, and our studies have demonstrated their ability to release the cargo protein while degrading slowly over 1 week, the 10% GelMA groups were selected for use in subsequent experiments. In our transwell studies, we first confirmed that liposomal encapsulation of the protein does not negatively impact its ability to chemoattract MSCs (Figures 5A and 5B). Media conditioned by either GelMA + SDF or GelMA + lipoSDF were then collected at days 0, 1, 3, and 7 to assess for the continued ability of the system to release chemokine capable of inducing cell migration. In the GelMA + lipoSDF group, we saw an increase in cell migration over time (Figure 5C), reflecting the exponential profile of protein release suggested by our modeling data. This exponential trend of release followed what we had observed from our release studies, suggesting that lipoSDF is a more tunable method of SDF-1α release that can predictably induce the migration of MSCs for up to 1

week. Conversely, no such trend was predicted by our models for the GelMA + SDF group and did not correlate with what was observed experimentally in our migration studies.

We also found that our nanocomposite hydrogel delivery system is capable of affecting the phosphorylation status of key proteins from the mTOR pathway, which is known to be stimulated by SDF-1α through the protein's cognate receptor CXCR4 [55–57]. While there are many highly complex signal transduction pathways that influence the behavior and function of cells, we opted to study the mTOR pathway in particular due to its role in stimulating cell metabolism, migration, and the production of pro-healing proteins [58,59]. Furthermore, mTOR signaling is associated with the regulation of glucose metabolism and is differentially regulated among pro- and anti-inflammatory subsets of immune cells due to their different metabolic demands [60,61].

For our work, we chose to study the levels of phosphorylated AKT, which is the biologically active form of the protein that activates mTOR [62]. We also chose to probe for levels of phosphorylated RPS6, which is further downstream mTOR and is implicated in protein synthesis [58]. In our Western blot experiments, we saw that GelMA + lipoSDF, but not GelMA + SDF, reached similar levels of phospho-AKT as the positive (free SDF-1α) control across all days (Figure 6B). Curiously, the levels of phospho-AKT for the free SDF-1α control were lower than that of the negative PBS control. This may be due to feedback inhibition of phospho-AKT by mTOR as signaling reaches equilibrium [56,58]. Alternatively, exposure to the released SDF-1α may have caused the cells to adopt a lower bioenergetic state with decreased mTOR activity, a phenomenon that has been previously observed in anti-inflammatory macrophages subtypes [61]. We also hypothesize that the variations between experiments may be due to nonspecific charge-charge interactions between GelMA and SDF-1α that may interfere with diffusion and binding of the protein to its receptor [12,13]. Similarly, the levels of phospho-RPS6 appeared to decrease slightly upon stimulation with free SDF-1α. In both our groups, we saw decreasing levels of phospho-RPS6 with time (Figure 6C), suggesting that the amount of released protein present at each time point was still capable of inducing mTOR signaling activity within MSCs at or beyond the capability of the positive control.

Overall, our studies indicate that our nanocomposite delivery system is capable of releasing and maintaining local concentrations of bioactive SDF-1α at levels capable of stimulating MSC recruitment *in vitro*. We were able to observe these effects for up to 1 week, which is a physiologically relevant *in vivo* timespan for the migration of MSCs and other local immunomodulatory cell types such as macrophages [63,64]. The results of this work represent a promising approach that expands on current strategies for the controlled delivery of therapeutic proteins, with important implications in biomedical research and development, as well as in clinical settings.

5. Conclusions

The healing progression and ultimate outcome of a wound are highly dependent on the activity of immunomodulatory cell populations such as MSCs. Chronic wounds in particular are characterized by persistent inflammation preventing the progression of normal healing

mechanisms that lead to wound closure and skin tissue regeneration [65,66]. This inflammatory microenvironment impairs the recruitment of MSCs that normally secrete immunomodulatory and pro-healing cytokines which play an important role in tissue repair [8,9]. In our work, we have demonstrated that we are able to fabricate a nanocomposite liposome-hydrogel system capable of stably encapsulating and tuning the release of the chemokine SDF-1α over time. We further show that this system is able to affect intracellular mTOR signaling as well as induce chemotaxis in MSCs. To our knowledge, this is the first study to report the delivery of liposomal SDF-1α using a nanocomposite strategy. We believe that this work could be in turn extended to the delivery of other therapeutic proteins or applied to clinical applications including wound healing, immunomodulation, and tissue regeneration.

Supplementary Material

Refer to Web version on PubMed Central for supplementary material.

Acknowledgements

This work was supported by the National Institute of Biomedical Imaging and Bioengineering/National Institutes of Health (NIBIB/NIH) Center for Engineering Complex Tissues (grant number P41 EB023833). The authors would like to thank Dr. Fu Chen for helping with sample acquisition using NMR, as well as Dr. Wen-An Chiou for assistance with cryoTEM and SEM imaging. JRY also gratefully acknowledges support from the University of Maryland School of Medicine.

References

[1]. Turner NJ, Badylak SF, The Use of Biologic Scaffolds in the Treatment of Chronic Nonhealing Wounds., Adv. Wound Care 4 (2015) 490–500. 10.1089/wound.2014.0604.

[2]. Han G, Ceilley R, Chronic Wound Healing: A Review of Current Management and Treatments, Adv. Ther 34 (2017) 599–610. 10.1007/s12325-017-0478-y. [PubMed: 28108895]

[3]. Rose JF, Giovinco N, Mills JL, Najafi B, Pappalardo J, Armstrong DG, Split-thickness skin grafting the high-risk diabetic foot, J. Vasc. Surg 59 (2014) 1657–1663. 10.1016/j.jvs.2013.12.046. [PubMed: 24518607]

[4]. Seyhan T, Split-Thickness Skin Graft, in: Spear M (Ed.), Ski. Grafts – Indic. Appl. Curr. Res, InTech, Rijeka, 2011: pp. 3–17. 10.5772/23658.

[5]. Debels H, Hamdi M, Abberton K, Morrison W, Dermal Matrices and Bioengineered Skin Substitutes, Plast. Reconstr. Surg. Glob. Open 3 (2015) 63–72. 10.1097/GOX.0000000000000219.

[6]. Burdick JA, Mauck RL, Biomaterials for tissue engineering applications: A review of the past and future trends, 2011 10.1007/978-3-7091-0385-2.

[7]. Madaghiele M, Sannino A, Ambrosio L, Demitri C, Polymeric hydrogels for burn wound care: Advanced skin wound dressings and regenerative templates, Burn. Trauma 2 (2014) 153 10.4103/2321-3868.143616.

[8]. Yu JR, Navarro J, Coburn JC, Mahadik B, Molnar J, Holmes JH, Nam AJ, Fisher JP, Current and Future Perspectives on Skin Tissue Engineering: Key Features of Biomedical Research, Translational Assessment, and Clinical Application, Adv. Healthc. Mater 8 (2019) 1801471 10.1002/adhm.201801471.

[9]. Xu F, Zhang C, Graves DT, Abnormal cell responses and role of TNF- α in impaired diabetic wound healing, Biomed Res. Int 2013 (2013) 754802 10.1155/2013/754802. [PubMed: 23484152]

[10]. Hocking AM, The Role of Chemokines in Mesenchymal Stem Cell Homing to Wounds., Adv. Wound Care 4 (2015) 623–630. 10.1089/wound.2014.0579.

[11]. Krieger JR, Ogle ME, McFaline-Figueroa J, Segar CE, Temenoff JS, Botchwey EA, Spatially localized recruitment of anti-inflammatory monocytes by SDF-1αreleasing hydrogels enhances microvascular network remodeling, Biomaterials. 77 (2016) 280–290. 10.1016/j.biomaterials.2015.10.045. [PubMed: 26613543]

[12]. Purcell BP, Elser JA, Mu A, Margulies KB, Burdick JA, Synergistic effects of SDF1α chemokine and hyaluronic acid release from degradable hydrogels on directing bone marrow derived cell homing to the myocardium, Biomaterials. 33 (2012) 7849–7857. 10.1016/j.biomaterials.2012.07.005. [PubMed: 22835643]

[13]. Dalonneau F, Liu XQ, Sadir R, Almodovar J, Mertani HC, Bruckert F, Albiges-Rizo C, Weidenhaupt M, Lortat-Jacob H, Picart C, The effect of delivering the chemokine SDF-1α in a matrix-bound manner on myogenesis., Biomaterials. 35 (2014) 4525–4535. 10.1016/j.biomaterials.2014.02.008. [PubMed: 24612919]

[14]. Kim YH, Tabata Y, Recruitment of mesenchymal stem cells and macrophages by dual release of stromal cell-derived factor-1 and a macrophage recruitment agent enhances wound closure, J. Biomed. Mater. Res. - Part A 104 (2016) 942–956. 10.1002/jbm.a.35635.

[15]. Hu C, Yong X, Li C, Lü M, Liu D, Chen L, Hu J, Teng M, Zhang D, Fan Y, Liang G, CXCL12/CXCR4 axis promotes mesenchymal stem cell mobilization to burn wounds and contributes to wound repair, J. Surg. Res (2013). 10.1016/j.jss.2013.01.019.

[16]. Braza F, Dirou S, Forest V, Sauzeau V, Hassoun D, Chesné J, Cheminant-Muller MA, Sagan C, Magnan A, Lemarchand P, Mesenchymal Stem Cells Induce Suppressive Macrophages Through Phagocytosis in a Mouse Model of Asthma, Stem Cells. 34 (2016) 1836–1845. 10.1002/stem.2344. [PubMed: 26891455]

[17]. de Witte SFH, Luk F, Sierra Parraga JM, Gargesha M, Merino A, Korevaar SS, Shankar AS, O'Flynn L, Elliman SJ, Roy D, Betjes MGH, Newsome PN, Baan CC, Hoogduijn MJ, Immunomodulation By Therapeutic Mesenchymal Stromal Cells (MSC) Is Triggered Through Phagocytosis of MSC By Monocytic Cells, Stem Cells. 36 (2018) 602–615. 10.1002/stem.2779. [PubMed: 29341339]

[18]. Prokoph S, Chavakis E, Levental KR, Zieris A, Freudenberg U, Dimmeler S, Werner C, Sustained delivery of SDF-1α from heparin-based hydrogels to attract circulating pro-angiogenic cells, Biomaterials. 33 (2012) 4792–4800. 10.1016/J.BIOMATERIALS.2012.03.039. [PubMed: 22483246]

[19]. Segers VFM, Tokunou T, Higgins LJ, MacGillivray C, Gannon J, Lee RT, Local Delivery of Protease-Resistant Stromal Cell Derived Factor-1 for Stem Cell Recruitment After Myocardial Infarction, Circulation. 116 (2007) 1683–1692. 10.1161/CIRCULATIONAHA.107.718718. [PubMed: 17875967]

[20]. Zhao X, Lang Q, Yildirimer L, Lin ZY, Cui W, Annabi N, Ng KW, Dokmeci MR, Ghaemmaghami AM, Khademhosseini A, Photocrosslinkable Gelatin Hydrogel for Epidermal Tissue Engineering, Adv. Healthc. Mater 5 (2016) 108–118. 10.1002/adhm.201500005. [PubMed: 25880725]

[21]. Wang Z, Wang Z, Lu WW, Zhen W, Yang D, Peng S, Novel biomaterial strategies for controlled growth factor delivery for biomedical applications, NPG Asia Mater. 9 (2017) e435 10.1038/am.2017.171.

[22]. Della Porta G, Nguyen BNB, Campardelli R, Reverchon E, Fisher JP, Synergistic effect of sustained release of growth factors and dynamic culture on osteoblastic differentiation of mesenchymal stem cells, J. Biomed. Mater. Res. - Part A 103 (2015) 2161–2171. 10.1002/jbm.a.35354.

[23]. Zhao F, Yao D, Guo R, Deng L, Dong A, Zhang J, Composites of Polymer Hydrogels and Nanoparticulate Systems for Biomedical and Pharmaceutical Applications, Nanomaterials. 5 (2015) 2054–2130. 10.3390/nano5042054. [PubMed: 28347111]

[24]. Gaharwar AK, Peppas NA, Khademhosseini A, Nanocomposite hydrogels for biomedical applications, Biotechnol. Bioeng 111 (2014) 441–453. 10.1002/bit.25160. [PubMed: 24264728]

[25]. Mufamadi MS, Pillay V, Choonara YE, Du Toit LC, Modi G, Naidoo D, Ndesendo VMK, A Review on Composite Liposomal Technologies for Specialized Drug Delivery, J. Drug Deliv 2011 (2011) 1–19. 10.1155/2011/939851.

[26]. Jain S, Patel N, Shah MK, Khatri P, Vora N, Recent Advances in Lipid-Based Vesicles and Particulate Carriers for Topical and Transdermal Application, J. Pharm. Sci 106 (2017) 423–445. 10.1016/J.XPHS.2016.10.001. [PubMed: 27865609]

[27]. Kuo C-Y, Eranki A, Placone JK, Rhodes KR, Aranda-Espinoza H, Fernandes R, Fisher JP, Kim PCW, Development of a 3D Printed, Bioengineered Placenta Model to Evaluate the Role of Trophoblast Migration in Preeclampsia, ACS Biomater. Sci. Eng 2 (2016) 1817–1826. 10.1021/acsbiomaterials.6b00031.

[28]. Kuo C-Y, Guo T, Cabrera-Luque J, Arumugasaamy N, Bracaglia L, Garcia-Vivas A, Santoro M, Baker H, Fisher J, Kim P, Placental basement membrane proteins are required for effective cytotrophoblast invasion in a three-dimensional bioprinted placenta model, J. Biomed. Mater. Res. Part A 106 (2018) 1476–1487. 10.1002/jbm.a.36350.

[29]. Bracaglia LG, Messina M, Winston S, Kuo CY, Lerman M, Fisher JP, 3D Printed Pericardium Hydrogels to Promote Wound Healing in Vascular Applications, Biomacromolecules. 18 (2017) 3802–3811. 10.1021/acs.biomac.7b01165. [PubMed: 28976740]

[30]. Narenji M, Talaee MR, Moghimi HR, Effect of charge on separation of liposomes upon stagnation, Iran. J. Pharm. Res 16 (2017) 423–431. http://www.ncbi.nlm.nih.gov/pubmed/28979297 (accessed December 4, 2018). [PubMed: 28979297]

[31]. Baglo Y, Liang BJ, Robey RW, Ambudkar SV, Gottesman MM, Huang HC, Porphyrin-lipid assemblies and nanovesicles overcome ABC transporter-mediated photodynamic therapy resistance in cancer cells, Cancer Lett. 457 (2019) 110–118. 10.1016/j.canlet.2019.04.037. [PubMed: 31071369]

[32]. Inglut CT, Gaitan B, Najafali D, Lopez IA, Connolly NP, Orsila S, Perttilä R, Woodworth GF, Chen Y, Huang H, Predictors and Limitations of the Penetration Depth of Photodynamic Effects in the Rodent Brain, Photochem. Photobiol (2019) php.13155. 10.1111/php.13155.

[33]. Huang HC, Rizvi I, Liu J, Anbil S, Kalra A, Lee H, Baglo Y, Paz N, Hayden D, Pereira S, Pogue BW, Fitzgerald J, Hasan T, Photodynamic priming mitigates chemotherapeutic selection pressures and improves drug delivery, Cancer Res. 78 (2018) 558–571. 10.1158/0008-5472.CAN-17-1700. [PubMed: 29187403]

[34]. Huang HC, Liu J, Baglo Y, Rizvi I, Anbil S, Pigula M, Hasan T, Mechanism-informed repurposing of minocycline overcomes resistance to topoisomerase inhibition for peritoneal carcinomatosis, Mol. Cancer Ther 17 (2018) 508–520. 10.1158/1535-7163.MCT-17-0568. [PubMed: 29167313]

[35]. Liang BJ, Pigula M, Baglo Y, Najafali D, Hasan T, Huang HC, Breaking the selectivity-uptake trade-off of photoimmunoconjugates with nanoliposomal irinotecan for synergistic multi-tier cancer targeting, J. Nanobiotechnology 18 (2020) 1 10.1186/s12951-019-0560-5. [PubMed: 31898555]

[36]. Ovsianikov A, Deiwick A, Van Vlierberghe S, Dubruel P, M€Oller L, Dr€ G, Chichkov B, Laser Fabrication of Three-Dimensional CAD Scaffolds from Photosensitive Gelatin for Applications in Tissue Engineering, Biomacromolecules. 12 (2011) 851–858. 10.1021/bm1015305. [PubMed: 21366287]

[37]. Hansen J, Platten F, Wagner D, Egelhaaf SU, Tuning protein–protein interactions using cosolvents: specific effects of ionic and non-ionic additives on protein phase behavior, Phys. Chem. Chem. Phys 18 (2016) 10270–10280. 10.1039/C5CP07285A. [PubMed: 27020538]

[38]. Venkiteswaran G, Lewellis SW, Wang J, Reynolds E, Nicholson C, Knaut H, Generation and dynamics of an endogenous, self-generated signaling gradient across a migrating tissue, Cell. 155 (2013) 674 10.1016/j.cell.2013.09.046. [PubMed: 24119842]

[39]. Cussler EL, Diffusion - Mass Transfer in Fluid Systems, Third Edition, 3rd ed., Cambridge University Press, Cambridge, UK, 2009.

[40]. Baishya H, Application of Mathematical Models in Drug Release Kinetics of Carbidopa and Levodopa ER Tablets, J. Dev. Drugs 06 (2017). 10.4172/23296631.1000171.

[41]. Costa P, Sousa Lobo JM, Modeling and comparison of dissolution profiles, Eur. J. Pharm. Sci 13 (2001) 123–133. 10.1016/S0928-0987(01)00095-1. [PubMed: 11297896]

[42]. Wickremasinghe NC, Kumar VA, Hartgerink JD, Two-Step Self-Assembly of Liposome-Multidomain Peptide Nanofiber Hydrogel for Time-Controlled Release, Biomacromolecules. 15 (2014) 3587–3595. 10.1021/bm500856c. [PubMed: 25308335]

[43]. Alemdaroğlu C, Degim Z, Celebi N, Şengezer M, Alömeroglu M, Nacar A, Investigation of epidermal growth factor containing liposome formulation effects on burn wound healing, J. Biomed. Mater. Res. Part A 85A (2008) 271–283. 10.1002/jbm.a.31588.

[44]. Olekson MAP, Faulknor R, Bandekar A, Sempkowski M, Hsia HC, Berthiaume F, SDF-1 liposomes promote sustained cell proliferation in mouse diabetic wounds, Wound Repair Regen. 23 (2015) 711–723. 10.1111/wrr.12334. [PubMed: 26110250]

[45]. Bader AR, Li T, Wang W, Kohane DS, Loscalzo J, Zhang Y-Y, Preparation and Characterization of SDF-1a-Chitosan-Dextran Sulfate Nanoparticles, J. Vis. Exp (2015) 448869 10.3791/52323.

[46]. Ternullo S, Basnet P, Holsæter AM, Flaten GE, de Weerd L, Škalko-Basnet N, Deformable liposomes for skin therapy with human epidermal growth factor: The effect of liposomal surface charge, Eur. J. Pharm. Sci 125 (2018) 163–171. 10.1016/j.ejps.2018.10.005. [PubMed: 30300691]

[47]. Nam M, Lee J, Lee KY, Kim J, Sequential Targeted Delivery of Liposomes to Ischemic Tissues by Controlling Blood Vessel Permeability, ACS Biomater. Sci. Eng 4 (2018) 532–538. 10.1021/acsbiomaterials.7b00815.

[48]. Dhoot NO, Wheatley MA, Microencapsulated liposomes in controlled drug delivery: Strategies to modulate drug release and eliminate the burst effect, J. Pharm. Sci 92 (2003) 679–689. 10.1002/jps.19104. [PubMed: 12587129]

[49]. Gainza G, Villullas S, Pedraz JL, Hernandez RM, Igartua M, Advances in drug delivery systems (DDSs) to release growth factors for wound healing and skin regeneration, Nanomedicine Nanotechnology, Biol. Med 11 (2015) 1551–1573. 10.1016/J.NANO.2015.03.002.

[50]. Yue K, Trujillo-de Santiago G, Alvarez MM, Tamayol A, Annabi N, Khademhosseini A, Synthesis, properties, and biomedical applications of gelatin methacryloyl (GelMA) hydrogels., Biomaterials. 73 (2015) 254–71. 10.1016/j.biomaterials.2015.08.045. [PubMed: 26414409]

[51]. Gao W, Vecchio D, Li J, Zhu J, Zhang Q, Fu V, Li J, Thamphiwatana S, Lu D, Zhang L, Hydrogel Containing Nanoparticle-Stabilized Liposomes for Topical Antimicrobial Delivery, ACS Nano. 8 (2014) 2900–2907. 10.1021/nn500110a. [PubMed: 24483239]

[52]. Young S, Wong M, Tabata Y, Mikos AG, Gelatin as a delivery vehicle for the controlled release of bioactive molecules, J. Control. Release 109 (2005) 256–274. 10.1016/J.JCONREL.2005.09.023. [PubMed: 16266768]

[53]. Dealwis C, Fernandez EJ, Thompson DA, Simon RJ, Siani MA, Lolis E, Crystal structure of chemically synthesized [N33A] stromal cell-derived factor 1alpha, a potent ligand for the HIV-1 “fusin” coreceptor., Proc. Natl. Acad. Sci. U. S. A 95 (1998) 6941–6. 10.1073/pnas.95.12.6941. [PubMed: 9618518]

[54]. Kolambkar YM, Dupont KM, Boerckel JD, Huebsch N, Mooney DJ, Hutmacher DW, Guldberg RE, An alginate-based hybrid system for growth factor delivery in the functional repair of large bone defects., Biomaterials. 32 (2011) 65–74. 10.1016/j.biomaterials.2010.08.074. [PubMed: 20864165]

[55]. Ryu CH, Park SA, Kim SM, Lim JY, Jeong CH, Jun JA, Oh JH, Park SH, Oh W, Jeun S-S, Migration of human umbilical cord blood mesenchymal stem cells mediated by stromal cell-derived factor-1/CXCR4 axis via Akt, ERK, and p38 signal transduction pathways, Biochem. Biophys. Res. Commun 398 (2010) 105–110. 10.1016/j.bbrc.2010.06.043. [PubMed: 20558135]

[56]. Cherla RP, Ganju RK, Stromal Cell-Derived Factor 1α-Induced Chemotaxis in T Cells Is Mediated by Nitric Oxide Signaling Pathways, J. Immunol 166 (2001) 3067–3074. 10.4049/jimmunol.166.5.3067. [PubMed: 11207257]

[57]. Kucia M, Jankowski K, Reca R, Wysoczynski M, Bandura L, Allendorf DJ, Zhang J, Ratajczak J, Ratajczak MZ, CXCR4–SDF-1 Signalling, Locomotion, Chemotaxis and Adhesion, J. Mol. Histol 35 (2003) 233–245. 10.1023/B:HIJO.0000032355.66152.b8.

[58]. Mendoza MC, Er EE, Blenis J, The Ras-ERK and PI3K-mTOR pathways: cross-talk and compensation, Trends Biochem. Sci 36 (2011) 320–328. 10.1016/j.tibs.2011.03.006. [PubMed: 21531565]

[59]. Xing W, Guo W, Zou CH, Fu TT, Li XY, Zhu M, Qi JH, Song J, Dong CH, Li Z, Xiao Y, Yuan PS, Huang H, Xu X, Acemannan accelerates cell proliferation and skin wound healing through AKT/mTOR signaling pathway, J. Dermatol. Sci 79 (2014) 101–109. 10.1016/j.jdermsci.2015.03.016.

[60]. Lech M, Anders HJ, Macrophages and fibrosis: How resident and infiltrating mononuclear phagocytes orchestrate all phases of tissue injury and repair, Biochim. Biophys. Acta - Mol. Basis Dis 1832 (2013) 989–997. 10.1016/j.bbadis.2012.12.001.

[61]. Vasandan AB, Jahnavi S, Shashank C, Prasad P, Kumar A, Prasanna SJ, Human Mesenchymal stem cells program macrophage plasticity by altering their metabolic status via a PGE2-dependent mechanism, Nat. Sci. Reports 6 (2016) 38308 10.1038/srep38308.

[62]. Yentrapalli R, Azimzadeh O, Sriharshan A, Malinowsky K, Merl J, Wojcik A, Harms-Ringdahl M, Atkinson MJ, Becker K-F, Haghdoost S, Tapio S, The PI3K/Akt/mTOR Pathway Is Implicated in the Premature Senescence of Primary Human Endothelial Cells Exposed to Chronic Radiation, PLoS One. 8 (2013) e70024 10.1371/journal.pone.0070024. [PubMed: 23936371]

[63]. Lee DE, Ayoub N, Agrawal DK, Mesenchymal stem cells and cutaneous wound healing: novel methods to increase cell delivery and therapeutic efficacy., Stem Cell Res. Ther 7 (2016) 37 10.1186/s13287-016-0303-6. [PubMed: 26960535]

[64]. Gurtner G, Werner S, Barrandon Y, Longaker M, Wound repair and regeneration, Nature. 453 (2008) 314–321. 10.1038/nature07039. [PubMed: 18480812]

[65]. Hesketh M, Sahin KB, West ZE, Murray RZ, Macrophage phenotypes regulate scar formation and chronic wound healing, Int. J. Mol. Sci 18 (2017). 10.3390/ijms18071545.

[66]. Armstrong D, McCulloch D, de Asla R, Management of Diabetic Foot Ulcers, UpToDate. (2018).

Statement of Significance

Chronic, non-healing wounds promote an inflammatory environment that inhibits the migration of mesenchymal stem cells (MSCs), which secrete pro-healing and regenerative cytokines. The goal of this project is to apply principles of tissue engineering to achieve controllable release of the pro-healing chemokine SDF-1α to modulate the intracellular signaling and migratory behavior of MSCs. In this work, we introduce a nanocomposite strategy to tailor the release of SDF-1α using a liposome/gelatin methacrylate hydrogel approach. We are the first group to report the delivery of liposomal SDF-1α using this strategy. Our findings aim to further elucidate the role of MSCs in directing wound healing and guide the development of immunomodulatory and therapeutic delivery strategies for clinical wound healing applications.

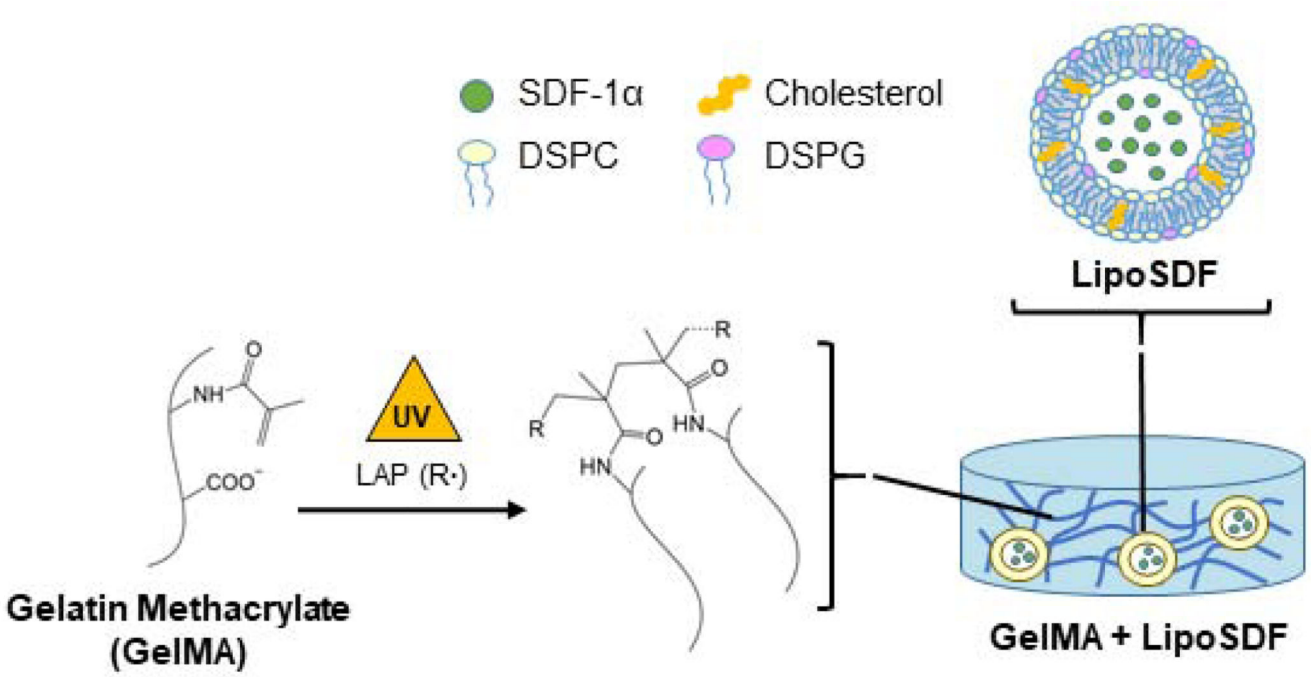

Figure 1: Strategy for SDF-1α delivery using a nanocomposite liposome/GelMA hydrogel.

Schematic of the overall delivery system, which is composed of liposomal SDF-1α (lipoSDF) loaded in a UV-crosslinkable gelatin methacrylate (GelMA) hydrogel derived from Type B gelatin. Anionic liposomes are formed by mixing DSPC, DSPG, and cholesterol at a 65:10:25 molar ratio.

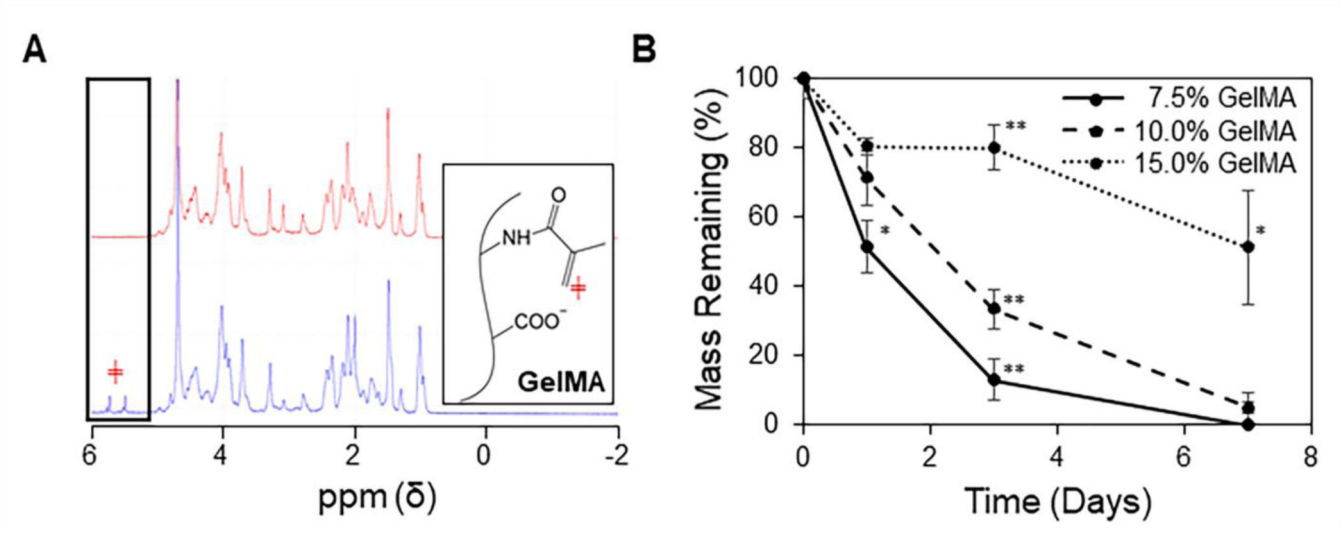

Figure 2: Characterization of the GelMA hydrogel.

(A) Representative 1H NMR spectrums of gelatin (red) and GelMA (blue), with the boxed peaks representing protons attached to the vinyl group of methacrylate (red ╪). (B) Degradation of GelMA hydrogels in collagenase IV shows a slower rate of degradation as GelMA content is increased (n = 3, mean ± STD). One-way ANOVAs with Tukey's post-hoc comparisons were conducted between groups at each time point. *$p < 0.005$ and **$p < 0.001$).

A

	Unloaded	Loaded
PdI	0.082 ± 0.0045	0.036 ± 0.019
EE (%)	N/A	87.8 ± 5.9
Diffusion Coefficient (cm^2/s)	2.09 ± 0.078 x 10^{-8}	2.01 ± 0.027 x 10^{-8}

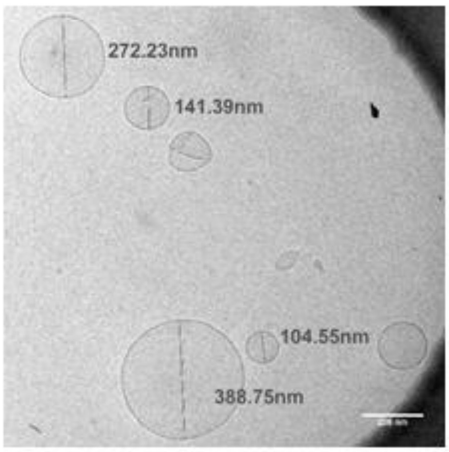

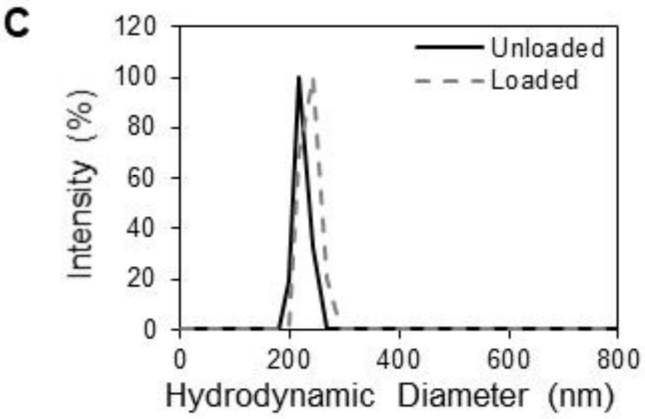

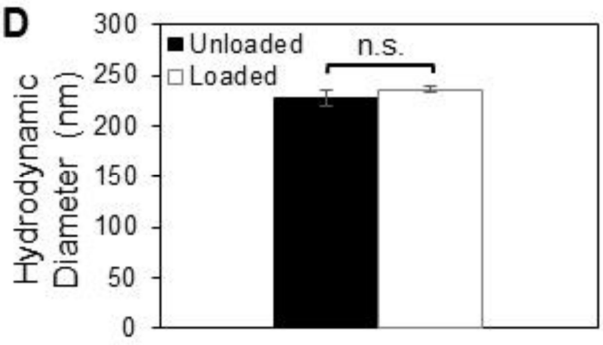

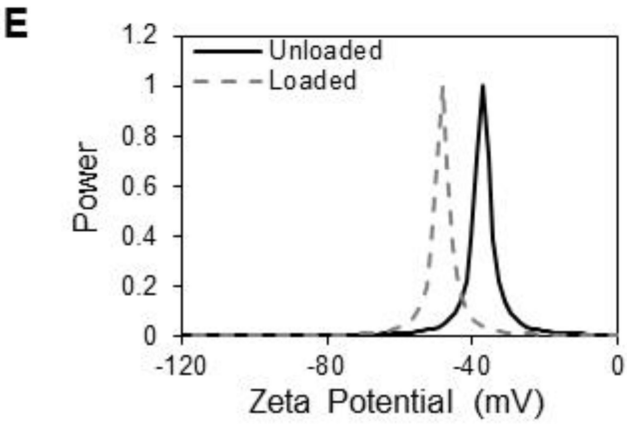

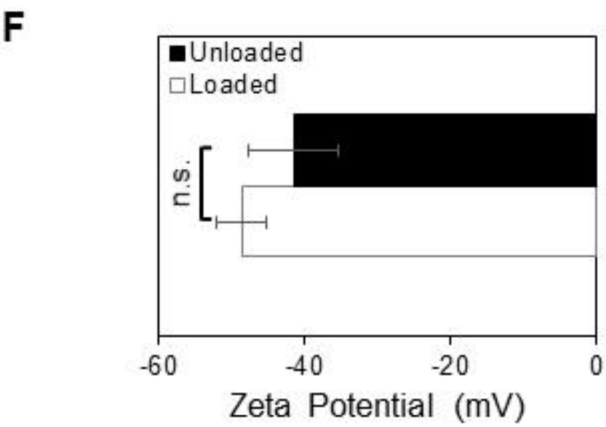

Figure 3: SDF-1α loaded into liposomes does not alter particle diameter or surface charge.

(A) Quantification of liposomal polydispersity index (PdI), encapsulation efficiency (EE%), and diffusion coefficients in water as measured by dynamic light scattering. (B) Cryo-TEM imaging of lipoSDF shows mostly spherical, unilamellar particles averaging around 200 nm in diameter (Scale bar: 200 nm). (C, D) Size and (E, F) zeta potential distributions of loaded and unloaded liposomes. The means between the two groups do not differ significantly (n = 3, mean ± STD. Student's T-test, $p > 0.05$). Each measurement was conducted with a different preparation of liposomes.

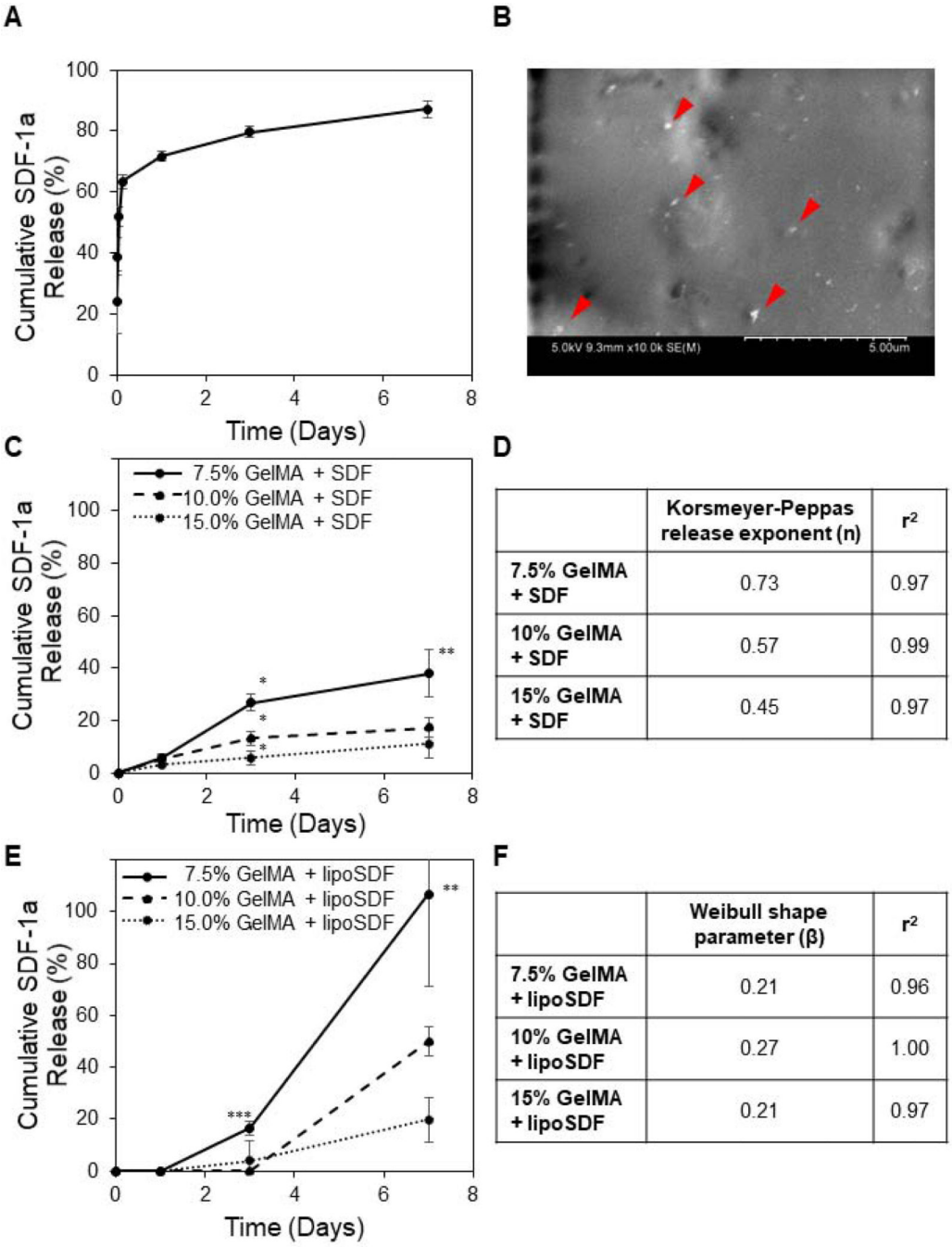

	Korsmeyer-Peppas release exponent (n)	r^2
7.5% GelMA + SDF	0.73	0.97
10% GelMA + SDF	0.57	0.99
15% GelMA + SDF	0.45	0.97

	Weibull shape parameter (β)	r^2
7.5% GelMA + lipoSDF	0.21	0.96
10% GelMA + lipoSDF	0.27	1.00
15% GelMA + lipoSDF	0.21	0.97

Figure 4: The release kinetics of SDF-1α can be tuned by incorporating the protein in a GelMA hydrogel.

(A) Cumulative SDF-1α released from liposomes over 1 week is characterized by burst release kinetics (n = 4, mean ± STD). (B) SEM imaging of GelMA + lipoSDF shows small particles of less than 500 nm dispersed throughout the surface of a hydrogel fiber (Scale bar: 5 μm). (C) Cumulative percentage of unencapsulated SDF-1α or (E) lipoSDF released from GelMA over 1 week, normalized to the amount of initial detectable protein (n = 4, mean ± STD). One-way ANOVAs with Tukey's post-hoc comparisons were conducted between groups at each time point. *$p < 0.0001$, **$p = 0.001$, ***$p < 0.01$). (D) Release exponent (n)

and r^2 values derived from the release of unencapsulated SDF-1α from GelMA hydrogels, fit to the Korsmeyer-Peppas model. (F) Shape parameter (β) and r^2 values derived from release of lipoSDF, fit to the Weibull release model.

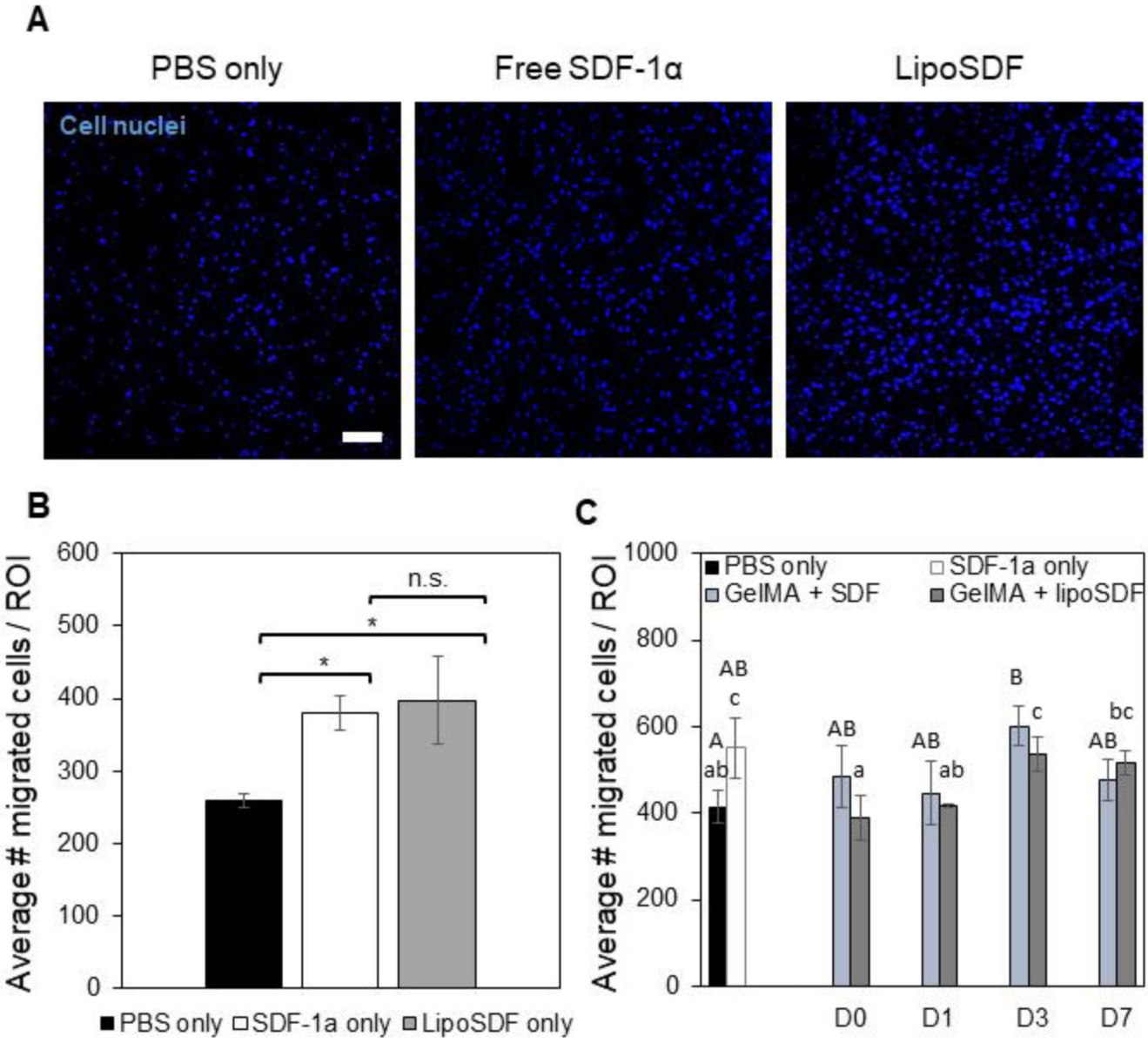

Figure 5: Liposomal encapsulation does not impair the chemotactic activity of SDF-1α and is able to induce chemotaxis for up to 1 week.

(A) Representative images and (B) quantitative cell counts from Hoechst-stained MSCs in a region of interest (ROI) that have migrated through a transwell membrane in response to the respective chemotactic factor: PBS, 80 ng/mL of free or liposomal SDF-1α (Scale bar: 100 μm. n = 3, mean ± STD. One-way ANOVAs with Tukey's post-hoc comparisons, *$p < 0.01$). (C) Comparison of MSC migration in response to media conditioned over 1 week by PBS, 80 ng/mL SDF-1α, or either 5 μg/mL of free or liposomal SDF-1α in 10% GelMA. Two sets of one-way ANOVAs with Tukey's post-hoc comparisons were conducted between groups (groups being compared are denoted by either upper- or lower-case letters). Groups that do not share a letter are statistically different ($p < 0.05$).

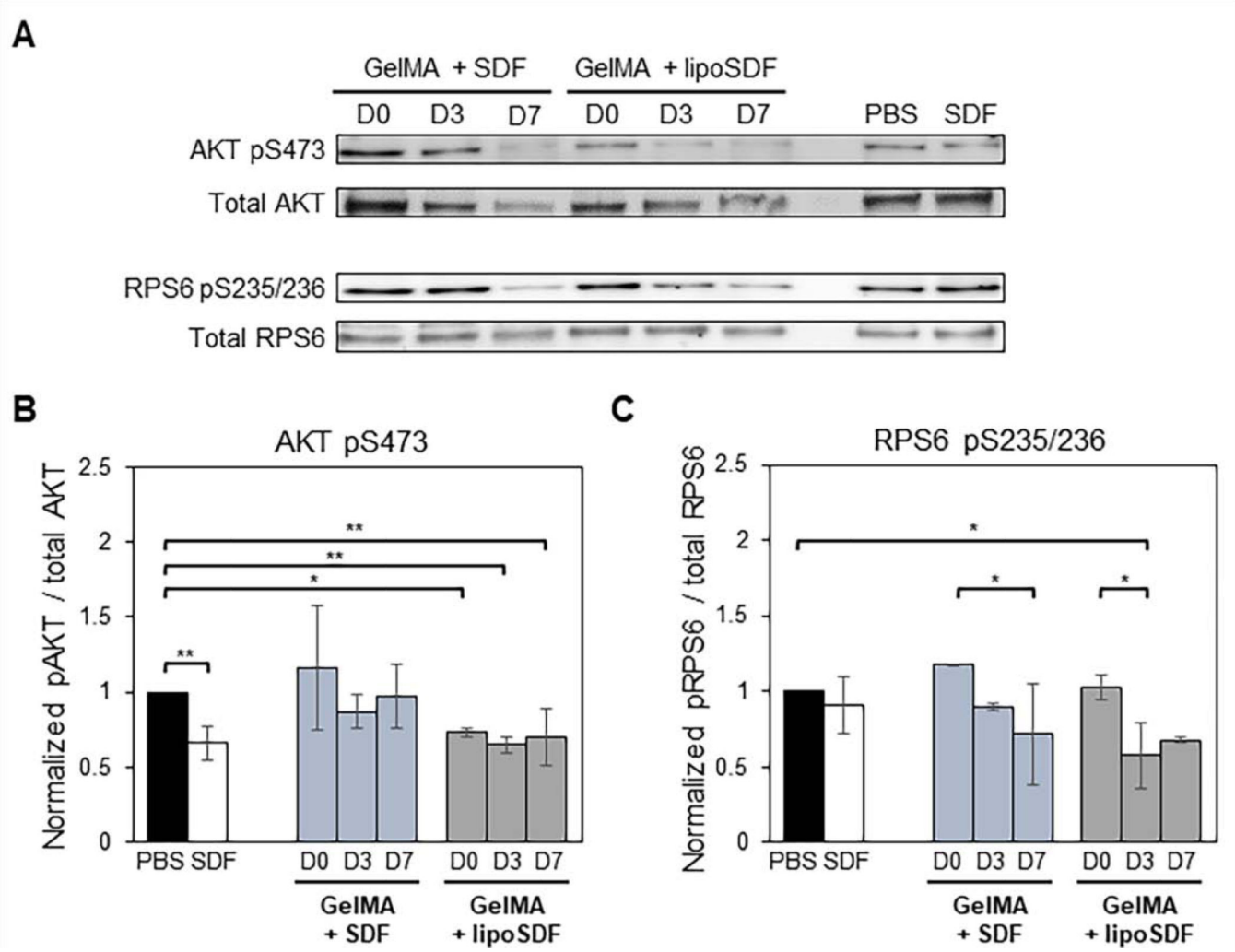

Figure 6: SDF-1α or lipoSDF in GelMA are capable of exerting effects on key proteins of the mTOR signaling pathway over 1 week.

(A) Representative Western blots of phosphorylated AKT and RPS6 compared to their respective total protein controls in MSCs exposed to PBS, 80 ng/mL free SDF-1α, or 5 μg/mL of either free or liposomal SDF-1α in GelMA. (B) Densitometry analysis of phosphorylated AKT and (C) RPS6. (n = 3, mean ± STD. Two sets of one-way ANOVAs with Tukey's post-hoc comparisons were conducted between groups. *$p < 0.05$ and **$p < 0.01$)